Original Article

Targeted Genes Sequencing Identified a Novel 15 bp Deletion on *GJA8* in a Chinese Family with Autosomal Dominant Congenital Cataracts

Han-Yi Min[1], Peng-Peng Qiao[2,3,4], Asan[3,4], Zhi-Hui Yan[5], Hui-Feng Jiang[5], Ya-Ping Zhu[3,4], Hui-Qian Du[3,4], Qin Li[3,4], Jia-Wei Wang[3,4], Jie Zhang[3,4], Jun Sun[3,4], Xin Yi[3,4,6,7], Ling Yang[3,4]

[1]Department of Ophthalmology, Chinese Academy of Medical Sciences, Peking Union Medical College Hospital, Beijing 100730, China
[2]College of Life Sciences, University of Chinese Academy of Sciences, Beijing 100049, China
[3]Binhai Genomics Institute, BGI-Tianjin, BGI-Shenzhen, Tianjin 300308, China
[4]Tianjin Translational Genomics Center, BGI-Tianjin, BGI-Shenzhen, Tianjin 300308, China
[5]Key Laboratory of Systems Microbial Biotechnology, Tianjin Institute of Industrial Biotechnology, Chinese Academy of Sciences, Tianjin 300308, China
[6]BGI-Shenzhen, Shenzhen, Guangdong 518083, China
[7]Guangzhou Key Laboratory of Cancer Trans-Omics Research (GZ2012, NO348), BGI-Guangzhou, BGI-Shenzhen, Guangzhou, Guangdong 510006, China

Abstract

Background: Congenital cataract (CC) is the leading cause of visual impairment or blindness in children worldwide. Because of highly genetic and clinical heterogeneity, a molecular diagnosis of the lens disease remains a challenge.
Methods: In this study, we tested a three-generation Chinese family with autosomal dominant CCs by targeted sequencing of 45 CC genes on next generation sequencing and evaluated the pathogenicity of the detected mutation by protein structure, pedigree validation, and molecular dynamics (MD) simulation.
Results: A novel 15 bp deletion on *GJA8* (c.426_440delGCTGGAGGGGACCCT or p. 143_147delLEGTL) was detected in the family. The deletion, concerned with an in-frame deletion of 5 amino acid residues in a highly evolutionarily conserved region within the cytoplasmic loop domain of the gap junction channel protein connexin 50 (Cx50), was in full cosegregation with the cataract phenotypes in the family but not found in 1100 control exomes. MD simulation revealed that the introduction of the deletion destabilized the Cx50 gap junction channel, indicating the deletion as a dominant-negative mutation.
Conclusions: The above results support the pathogenic role of the 15 bp deletion on *GJA8* in the Chinese family and demonstrate targeted genes sequencing as a resolution to molecular diagnosis of CCs.

Key words: Congenital Cataract; *GJA8*; Next Generation Sequencing; Novel In-frame Deletion; Targeted Genes Capture

Introduction

Congenital cataract (CC) refers to cataract observable at early year of life[1] and is the leading cause of visual losses in children worldwide.[2,3] The incidence of CC varies from 0.01% to 0.06% in developed countries[4] to 0.05–0.15% in less developed areas of the world.[2,3,5,6] CC can occur in isolation forms (nonsyndromic CC) or as part of a syndrome of ocular or systemic anomalies (syndromic CC).[7] Major causing factors of CC include metabolic disorders, intrauterine infectious, and genetic defects (chromosomal abnormalities or gene defects). Moreover, approximately 8.3–25.0% of the CC cases are thought to have a genetic basis of etiology, a majority of which are Mendelian diseases caused by monogenic mutations.[8,9]

CC is a group of clinically and genetically heterogeneous diseases. Clinically, in addition to other abnormalities

Access this article online

Quick Response Code:

Website: www.cmj.org

DOI: 10.4103/0366-6999.178966

Address for correspondence: Dr. Han-Yi Min, Department of Ophthalmology, Chinese Academy of Medical Sciences, Peking Union Medical College Hospital, Beijing 100730, China
E-Mail: wredge@sohu.com

Received: 23-11-2015 **Edited by:** Yi Cui
How to cite this article: Min HY, Qiao PP, Asan, Yan ZH, Jiang HF, Zhu YP, Du HQ, Li Q, Wang JW, Zhang J, Sun J, Yi X, Yang L. Targeted Genes Sequencing Identified a Novel 15 bp Deletion on *GJA8* in a Chinese Family with Autosomal Dominant Congenital Cataracts. Chin Med J 2016;129:860-7.

in syndromic CC, cataract itself includes a variety of morphologies, such as sutural, pulverulent, whole lens, nuclear, lamellar (also referred to as perinuclear), cortical, polar, cerulean, coralliform, and others.[9,10] Genetically, over 110 genes have been found associated with CC,[11] including more than 20 genes involved in nonsyndromic CC (hitherto the initial of the study).[9] Inherited patterns of nonsyndromic CC includes autosomal dominant (AD), autosomal recessive, and X-linked dominant patterns, with AD as the most common forms.[1,10] Of the more than 29 known nonsyndromic CC genes, at least 22 are involved in autosomal dominant congenital cataract (ADCC), including *BEST1*, *BFSP2*, *CHMP4B*, *CRYAA*, *CRYAB*, *CRYBA1*, *CRYBA4*, *CRYBB1*, *CRYBB2*, *CRYBB3*, *CRYGC*, *CRYGD*, *CRYGS*, *EPHA2*, *GJA3*, *GJA8*, *HSF4*, *MAF*, *MIP*, *PITX3*, *SLC16A12*, and *VIM*. Most of the genes mainly involve in specific processes in lens development, intercellular communication in the lens, or the organization of lens fibers.[9] Of note, the relation between cataract phenotypes and mutant genes is even more complex for nonsyndromic CC, i.e., mutations in different genes can cause similar cataracts phenotypes, mutations in a single gene can cause different types of cataracts, and one single mutation in a gene can cause different cataract phenotypes in patients.

Identifying the precise genetic cause of CC is essential for providing accurate diagnostics for medical management, prognostics, and recurrence risk counseling for the patient and family.[12] However, due to the highly clinical and genetic heterogeneity, clinical genetic diagnostic practice of CC, especially for nonsyndromic CC, is greatly limited with the traditional sequencing method which sequences a few candidate genes at each time. Despite this, recently, the next generation sequencing (NGS) combined with targeted genomic enrichment has proved to be a cost-effective resolution to the genetic test of genetically heterogeneous diseases and provide a new opportunity for genetic diagnostics of CC.

In this study, we performed parallel sequencing of 45 CC genes by combined NGS and targeted genomic enrichments to determine the genetic mutations in a three-generation Chinese family with congenital nuclear cataracts. We identified a novel c.426_440delGCTGGAGGGGACCCT in *GJA8* that segregates with the disease phenotype in the family and evaluated potential pathogenicity of the deletion and modeled the functional impacts of the deletion on the structure of the connexin 50 (Cx50) protein. Our result demonstrates that the targeted gene sequencing using NGS can be used as an effective tool for molecular diagnosis of CC.

Methods

Participants recruitment, blood sampling, and DNA extraction

This study was approved by the Institutional Review Boards of Beijing Genomic Institute (BGI)-Shenzhen. Nine members of a three-generation Chinese family from Guangdong with ADCCs were recruited in this study [Figure 1]. Careful ophthalmological examinations and hospital medical record reviews were performed for each affected member to confirm the clinical diagnosis. After obtained written informed consent, peripheral venous blood samples were collected for all participants. Genomic DNA was extracted using a QIAamp DNA Blood MiNi kit (Qiagen, Germany).

Capture probes design, targeted capture, and next generation sequencing

Forty-five genes implicated in the CC, including 29 nonsyndromic cataract genes (*AGK*, *BEST1*, *BFSP1*, *BFSP2*, *CHMP4B*, *CRYAA*, *CRYAB*, *CRYBA1*, *CRYBA4*, *CRYBB1*, *CRYBB2*, *CRYBB3*, *CRYGC*, *CRYGD*, *CRYGS*, *EPHA2*, *FYCO1*, *GJA3*, *GJA8*, *HSF4*, *P3H2*, *LIM2*, *MAF*, *MIP*, *NHS*, *PITX3*, *SLC16A12*, *TDRD7*, and *VIM*) and 16 syndromic cataract genes (*ABHD12*, *CNBP*, *CTDP1*, *EYA1*, *FTL*, *GALK1*, *GCNT2*, *GFER*, *GJA1*, *JAM3*, *OPA3*, *PAX6*, *RAB3GAP2*, *SIL1*, *SIX6*, and *SLC33A1*), were collected from careful literature and database search. The 45 genes selected contain almost all of the genes related to CC.[1,13] Moreover, genes related to ADCC, which are interested, were all included. Targeted sequencing capture DNA Probes were designed for exons and the flanking 30 bp intronic sequences using the Nimblegen SeqCap EZ Choice system (Roche NimbleGen, Madison, WI, USA). Targeted sequences capture and sequencing library preparation were performed as previously described.[14] Paired-end sequencing (PE100) was performed on the Illumina HiSeq2000 platform (Illumina, San Dieago, CA, USA).

Short-reads mapping, variant detection, and annotation

After filtering of reads of low-quality and potential adaptor contamination,[15] the clean reads were mapped to the reference human genome (hg19) using BWA software package (Burrows Wheeler Aligner http://sourceforge.net/projects/bio-bwa/).[16] Single nucleotide variants (SNVs) were identified using SOAPsnp software (http://soap.genomics.org.cn/),[17] and small insertion and deletions (InDels) were identified using the GATK InDel Genotyper (The Genome Analysis Toolkit, http://www.broadinstitute.org/gsa/wiki/index.php/).[18] The variants were annotated using a BGI in-house developed annotation pipeline.

Sequence conservation analysis and estimation of deleteriousness

Multiple alignments of Cx50 protein sequences between species were directly obtained from the UCSC genome browser home (http://genome.ucsc.edu/) and realigned with the Molecular Evolutionary Genetics Analysis (MEGA 6.06, http://www.megasoftware.net). The online free tool Combined Annotation-Dependent Depletion (CADD, http://cadd.gs.washington.edu/),[19] a newly developed framework that integrates diverse annotations into a single quantitative score (C-score) to measure the deleteriousness of SNVs and small InDels, was used to evaluate the pathogenicity of the deletion.

Construction of connexin 50 three-dimensional structure model

In the absence of Cx50 experimental structures, the comparative modeling methods based on high sequence identity can be employed to predict the Cx50 protein

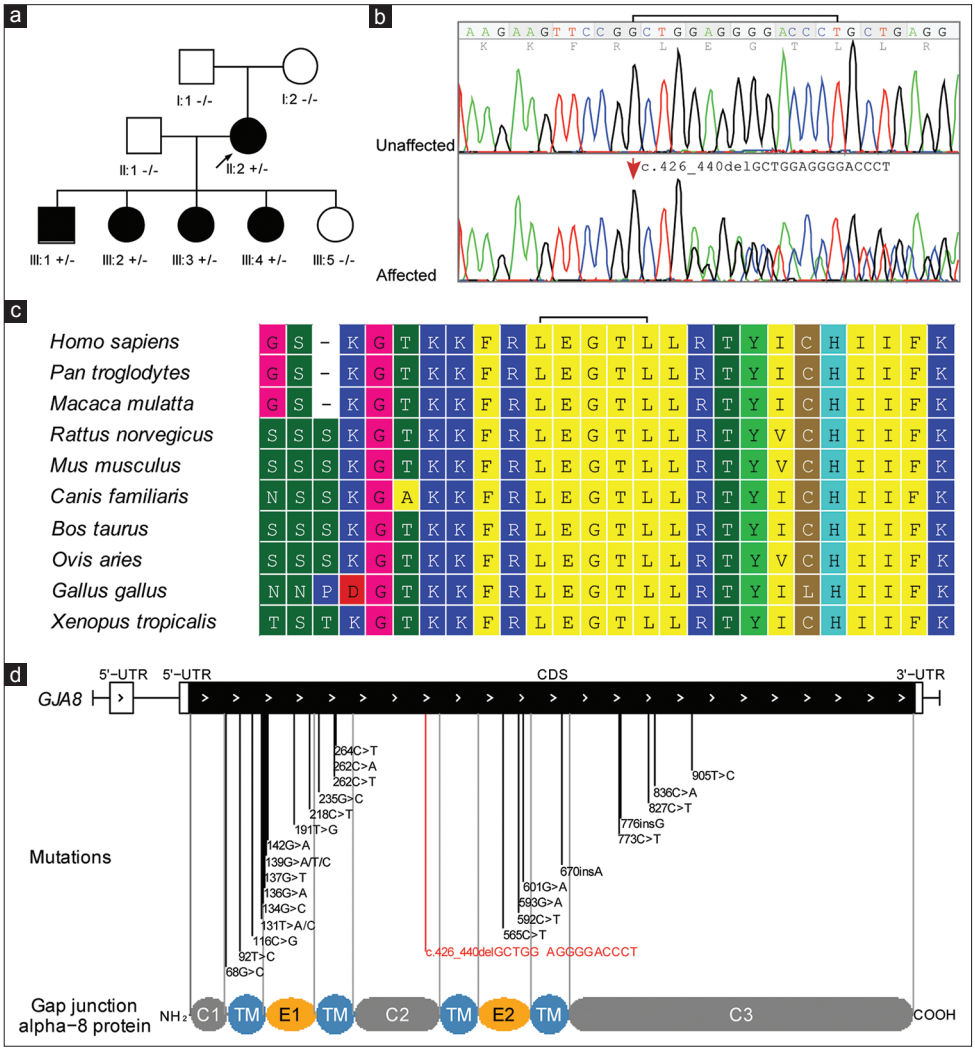

Figure 1: Pedigree and mutation analysis. (a) Pedigree of a three-generation Chinese family with congenital cataracts. The proband is indicated with an arrow. Squares and circles symbolize male and female individual, respectively. Black symbol indicates cataract affected status and white symbol indicates unaffected status. (b) DNA sequence chromatogram analysis. DNA sequence chromatograms of the unaffected members (top) and affected members (bottom) in the pedigree. Fifteen bases deletion in exon 2 causes a conservative deletion of LEGTL from codon 143–147 (p.143_147del). (c) Evolutionary sequence conservation analysis. Multiplex sequence alignment of connexin 50 from different species reveals that codon 143–147, where the mutation (p.143_147del) occurred, is located within a highly conserved region. (d) Allelic spectrum of reported disease-associated mutations. Schematic diagram of genomic structure of human *GJA8* gene and allelic spectrum of diseases mutations are shown. The identified mutation in this study is marked with red line. CL (C1/ C2/ C3): cytoplasmic loop domain; TM: transmembrane domain; E1:extracellular domain 1; E2: extracellular domain 2.

structure, which can subsequently be used to aid in the understanding of protein functional mechanisms. The amino acid sequences of wild type (WT) Cx50 and mutant Cx50 above were used to perform the sequence similarity searches using the NCBI BLAST in SWISS-MODEL server (http://swissmodel.expasy.org/).[20] The newly disclosed structure of human Cx26 (Protein Data Bank [PDB] code: 2ZW3)[21] was selected as the template to construct the Cx50 structure that shares a sequence identity of 57% with WT Cx50 sequence. The modeling result is shown in Supplementary Figure 1.

The system of generating lipid bilayer structures as well as membrane-bound protein structures, CHARMM-GUI Lipid Builder[22] was used to build a Cx50 protein/membrane complex for molecular dynamics (MD) simulations. The Cx50 models (WT and mutant) were inserted into a fully hydrated palmitoyl-oleyl phosphatidylcholine (POPC) lipid bilayer of 400 molecules (set 200 on the lower leaflet and 200 on the upper leaflet) [Supplementary Figure 2]. The water model used was three-point model (TIP3P). To remove the net charge of the system, an ionic concentration of 150 mM KCl by transmuting random water molecules into K^+ and Cl^- was added as counterions.

Molecular dynamics simulation

MD simulations were carried out using the parallel MD program GROMACS 4.6.5 for all protein molecules, POPC lipid molecules, and ions along with the TIP3P model for water molecules. A cutoff of 10 Å for van der Waals interactions was imposed. The particle mesh Ewald[23]

technique with a short-range cutoff of 10 Å was employed to calculate long-range electrostatic forces. The periodic boundary conditions were introduced on all simulations with an integration time step of 2 fs to employ a multiple time stepping algorithms. The simulations were equilibrated as an NPT ensemble, using the Langevin dynamics[24] method to keep the pressure at 1 atm, and the temperature was maintained at 303 K using Langevin dynamics with a very weak friction coefficient. The MD simulation protocol is detailed description as follows: To remove the largest strains in the system, all simulation systems were first subjected to 5000 cycles of steepest descent, while position restraints were applied to the residues of the Cx50 models as well as the molecules of POPC lipid bilayer. Afterward, MD with position restraints applied only to the protein was performed for 0.1 ns. All the positional restraints were eliminated in the third round, and the systems were allowed to preequilibrate for 5 ns. The production simulations were finally conducted for 10 ns for all systems.

Sanger sequencing

Polymerase chain reaction (PCR) primer sets were designed to sequence the first exons of *MAF, EPHA2*, and *NHS* genes not covered in targeted sequencing, as well as to analyze the segregation of the *GJA8* deletion in the family [Supplementary Table 1]. The PCR amplification was conducted in a 25 μl reaction volume containing 1X PCR buffer with 1.5 mM $MgCl_2$, 200 μM each dNTP, 0.25 U Taq DNA polymerase (Takara, Dalian, China), 1.5 μM primers, and 50 ng genomic DNA. The PCR condition was 94°C for 4 min, 35 cycles of 94°C for 30 s, 59°C for 30 s, and 72°C for 45 s, and a final 72°C for 10 min. The PCR products were purified and sequenced at both ends on an ABI3730xl DNA sequencer (PE Applied Biosystems, Forest City, CA, USA).

Results

Pedigree and clinical features

The family includes 5 affected and 4 unaffected members in a three-generation pedigree [Figure 1a]. The transmission of cataract from the female founder (also the proband) to four out of five of her offsprings with both genders supports a dominant inheritance pattern of the lens diseases in the family. All affected members have nuclear cataracts with no other ocular or systemic abnormalities [Figure 1a and Table 1]. The presences of cataracts at birth were confirmed by hospital records, and nonsyndromic CC was diagnosed for all affected members.

Targeted sequencing of 45 cataract genes

The coding sequence-exons and adjacent intronic sequences of 45 cataract genes, consisting of 366 exons and 63003 bp, were captured and sequenced for the proband DNA (see Materials and Methods). A total of 224,437 clean reads in 15,940,353 bp length (or ~15.94 Mb data) mapped to targeted regions were generated on Hiseq2000 [Table 2]. This formed a mean coverage depth of 218-fold on the targeted regions of the 45 cataract genes, with a general sequence coverage rate of 99.23% and a high-quality genotype assignment (>×10) rate of 97.29% [Table 2]. The uncovered targeted regions were all the first coding exons with extreme GC content [mean CC% >69%, Supplementary Table 2]. Supplementary sequencing was performed to cover the sequences of three of the uncovered first coding exons (see Materials and Methods) while the others were excluded for the analysis considering a syndromic form or a nondominant inheritance pattern of cataracts associated with the related genes [Supplementary Table 2].

Identification of potential causal mutation

Mapped against the human reference genome sequences, a total of 43 variants, including forty substitutes and 3 small InDels, were identified on the 45 genes [Table 3 and Supplementary Table 3]. A vast majority of these variants (29/43) were either synonymous substitutes or from untranslated regions [Table 3]. These variants are thought to be of less potentially pathogenicity, and we put them aside first. Of the remaining variants with potential function importance (including ten nonsynonymous, 3 splice acceptor and donor site mutations, and 1 coding InDels), only the heterozygous in-frame coding on *GJA8* was novel meeting the criteria as nonpolymorphic with an allele frequency <5% in any of the single nucleotide polymorphism database, HapMap, or 1000 genome project database. Multiplex protein sequences alignment shows that the deleted sequence was evolutionarily conserved among ten species with high-quality reference genome sequences available on UCSC genomes database [Figure 1c]. More importantly, the deletion was found in full cosegregation with cataract phenotypes in Sanger sequencing analysis of the mutation in the pedigree [Figure 1a and 1b] but was not detected in

Table 1: Summary of clinical evaluations for the Chinese cataract family

Member	Gender	Age at onset	Age at diagnosis	Cataract phenotypes	Other abnormalities	Diagnosis
I:1	Male	No	65	Normal	No	Normal
I:2	Female	No	67	Normal	No	Normal
II:1	Male	No	48	Normal	No	Normal
II:2	Female	On birth	42	Nuclear, bilateral	No	Congenital nuclear cataract
III:1	Male	On birth	13	Nuclear, bilateral	No	Congenital nuclear cataract
III:2	Female	On birth	22	Nuclear, bilateral	No	Congenital nuclear cataract
III:3	Female	On birth	25	Nuclear	No	Congenital nuclear cataract
III:4	Female	On birth	15	Nuclear	No	Congenital nuclear cataract
III:5	Female	On birth	18	Normal	No	Normal

Table 2: Summary statistics for targeted sequencing of 45 cataracts genes in the proband

Gene	OMIM diseases	Transcript	Number of coding exons	Sizes (bp)	Sequencing depth (X)	Coverage rate (%)		
						>1X	>4X	>10X
ABHD12	#612674 (AR, Sa)	NM_015600.4	13	1215	192	99.26	84.28	84.28
AGK	#614691 (AR, NSa)	NM_018238.3	16	1269	270	100.00	100.00	100.00
BEST1	#193220 (AD, NS)	NM_001139443.1	9	1815	320	100.00	100.00	100.00
BFSP1	#611391 (AR, NS)	NM_001195.3	8	1998	272	99.95	97.00	85.44
BFSP2	#611597 (AD, NS)	NM_003571.2	7	1248	164	100.00	100.00	100.00
CHMP4B	#605387 (AD, NS)	NM_176812.4	5	675	214	100.00	100.00	100.00
CNBP	#602668 (AD, S)	NM_001127192	4	513	155	97.87	94.92	93.94
CRYAA	#604219 (AD, NS)	NM_000394.2	3	522	154	100.00	100.00	100.00
CRYAB	#613763 (AD/AR, NS)	NM_001885.1	3	528	313	100.00	100.00	100.00
CRYBA1	#600881 (AD, NS)	NM_005208.4	6	648	245	100.00	100.00	100.00
CRYBA4	#610425(AD/AR, NS)	NM_001886.2	6	591	141	100.00	100.00	100.00
CRYBB1	#611544 (AD/AR, NS)	NM_001887.3	6	759	145	100.00	100.00	100.00
CRYBB2	#601547 (AD, NS)	NM_000496.2	6	618	194	100.00	100.00	100.00
CRYBB3	#609741 (AD/AR, NS)	NM_004076.3	6	636	144	100.00	100.00	100.00
CRYGC	#604307 (AD, NS)	NM_020989.3	3	525	179	100.00	100.00	100.00
CRYGD	#115700 (AD, NS)	NM_006891.3	3	525	179	100.00	100.00	100.00
CRYGS	#116100 (AD, NS)	NM_017541.2	3	537	364	100.00	100.00	100.00
CTDP1	#604168 (AR, S)	NM_004715.4	13	2886	126	92.31	89.12	89.12
EPHA2	#116600 (AD, NS)	NM_004431.3	17	2931	150	100.00	97.10	97.10
EYA1	#113650 (AD, S)	NM_000503.4	18	1779	314	100.00	100.00	100.00
FTL	#600886 (AD, S)	NM_000146.3	4	528	131	100.00	100.00	100.00
FYCO1	#610019 (AR, NS)	NM_024513.3	18	4437	194	100.00	100.00	100.00
GALK1	#230200 (AR, S)	NM_000154.1	8	1179	80	100.00	100.00	100.00
GCNT2	#110800 (AR, S)	NM_145649.4	5	1209	421	100.00	100.00	100.00
GFER	#613076 (AR, S)	NM_005262.2	3	618	120	100.00	95.63	73.46
GJA1	#257850 (AR, S)	NM_000165.3	2	1149	371	100.00	100.00	100.00
GJA3	#601885 (AD, NS)	NM_021954.3	2	1308	127	100.00	100.00	100.00
GJA8	#116200 (AD, NS)	NM_005267.4	2	1302	270	100.00	100.00	100.00
HSF4	#116800 (AD, NS)	NM_001040667.2	15	1479	125	100.00	100.00	98.24
JAM3	#613730 (AR, S)	NM_032801.4	9	933	275	100.00	100.00	100.00
LEPREL1	#614292 (AR, NS)	NM_018192.3	15	2127	191	100.00	99.76	92.57
LIM2	#615277 (AR, NS)	NM_030657.3	5	648	166	100.00	100.00	100.00
MAF	#610202 (AD, NS)	NM_005360.4	2	1212	100	79.04	76.32	73.10
MIP	#615274 (AD, NS)	NM_012064.3	4	792	204	100.00	100.00	100.00
NHS	#302200 (XD, NS and S)	NM_198270.2	8	4893	355	97.06	95.26	90.88
OPA3	#165300 (AD, S)	NM_001017989.2	2	543	75	100.00	100.00	100.00
PAX6	#106210 (AD, S)	NM_001258462.1	14	1311	283	100.00	100.00	100.00
PITX3	#610623 (AD, NS)	NM_005029.3	4	909	59	100.00	100.00	100.00
RAB3GAP2	#212720 (AR, S)	NM_012414.3	35	4182	327	100.00	100.00	100.00
SIL1	#248800 (AR, S)	NM_001037633.1	11	1386	193	100.00	100.00	100.00
SIX6	#212550 (AR, S)	NM_007374.2	2	741	206	100.00	100.00	100.00
SLC16A12	#612018 (AD, NS)	NM_213606.3	8	1551	334	100.00	100.00	100.00
SLC33A1	#614482 (AR, S)	NM_004733.3	6	1650	391	100.00	100.00	100.00
TDRD7	#613887 (AR, NS)	NM_014290.2	17	3297	368	100.00	100.00	100.00
VIM	#116300 (AD, NS)	NM_003380.3	10	1401	201	100.00	100.00	100.00
Total			366	63,003	218	99.23	98.43	97.29

OMIM: Online Mendelian Inheritance in Man; AR: Autosomal recessive; AD: Autosomal dominant; XD: X-linked dominant; S: Syndromic; NS: Non-syndromic.

1100 BGI in-house control exomes [Supplementary Table 3], genetically suggesting a potential pathogenic role of the deletion. Intriguingly, the deletion was not detected on both unaffected parents of the proband in Sanger sequencing validation analysis [Figure 1a and 1b], supporting a *de novo* occurrence of the deletion in the proband.

The pathogenicity of the deletion was further evaluated with CADD. The C-score of 15.52 supports a pathogenic role of the deletion (mutations with C-score >15 were supposed to be pathogenic).[19]

This novel heterozygous deletion was concerned with a sequence deletion of 5 amino acids (or 15 bp) at the

intracellular loop domain (cytoplasmic loop [CL]) of the Cx50 protein (or *GJA8*) [Figure 1d], which connects two transmembrane domains and was suspected to serving as binding sites of Ca^{2+}/CaM in gap junction channel function.[25,26] Mutations on *GJA8* have caused multiplex ADCCs (Cataract 1, multiple types, OMIM#116200) including nuclear cataracts.

Potential functional impact of the deletion

To illustrate the dysfunction of Cx50 mutant, we performed MD simulation. At first, the best hit in PDB of Cx50 protein was used to predict the three-dimensional structure (see Materials and Methods). The overall structure of Cx50 represents a typical channel protein that contains a hydrophobic surface and hydrophilic channel [Supplementary Figure 1]. Then, the protein/membrane complex with lipid bilayer system and water was built to simulate the environment of Cx50 in cell. Both WT and mutant of Cx50 were inserted into the lipid bilayer system [Figure 2a and Supplementary Figure 2].

Table 3: Summary statistics for variants detected in targeted sequencing of 45 cataract genes in the proband

Mutation type	Number
SNVs	40
NS	10
Synonymous	28
SS	2
InDels	3
Coding (I)	1
SS	1
UTR	1
NS/SS/I	14
Allele frequency ≤0.05 in dbSNP (snp137), HapMap or 1000 genomes project	2
Allele frequency ≤0.05 in 1100 BGI in-house control exomes	1
Frequency ≤0.05 in either	1

NS: Nonsynonymous; SS: Spicing sites; UTR: Untranslated regions; dbSNP: Single nucleotide polymorphism database; BGI: Beijing Genomic Institute; SNVs: Single nucleotide variants; InDels: Insertion and deletions.

Finally, MD simulation was performed on both models (see Methods). As shown in Figure 2b, WT protein molecules were very stable in our system. However, the mutant molecules were more dynamic and the root-mean-square deviation increased when mutant molecules stay in the system for a longer time. Thus, the mutant Cx50 becomes unstable in the simulated system, which may also happen in real cellular environment.

Discussion

The lens of human eye is an avascular structure, and gap junction channels encoded by Cxs function as the passage of intercellular transport of the ions and low molecular weight biomolecules. Cx50 (*GJA8*) and Cx46 (*GJA3*) are the major components of mammalian lens fiber cells, and mutations of these two genes account for approximately 20% of nonsyndromic familial cataract cases.[7] The typical structure of Cx includes a cytoplasmic N-terminal domain (NT), four transmembrane domains (TM1 to TM4), two extracellular loops (E1 and E2), a CL between TM2 and TM3, and a C-terminal domain (CT). In this study, we identified a novel in-frame deletion of 15 bp in the coding region of *GJA8* gene (c.426_440delGCTGGAGGGGACCCT) associated with CCs in a three-generation Chinese family by targeted genes sequencing.

Several lines of evidence support a pathogenic role of the deletion. First, the deletion was concerned with an in-frame deletion of 5 amino acids within a highly evolutionarily conserved region in the CL domain of Cx50 protein, which binds Ca^{2+}/CaM to mediate gap junction channel in the lens of the eye.[25,26] Second, the deletion was fully cosegregated with cataracts in the family but was not found in 1100 control exomes. Third, the cataract morphology of the affected members and inheritance pattern of the cataracts in the family were compatible with those of cataract caused by *GJA8* mutations. Fourth, deleteriousness evaluation with CADD supported pathogenicity of the deletion. Fifth, protein structure modeling revealed that mutant protein disrupts the structure stability of Cx50 channel.

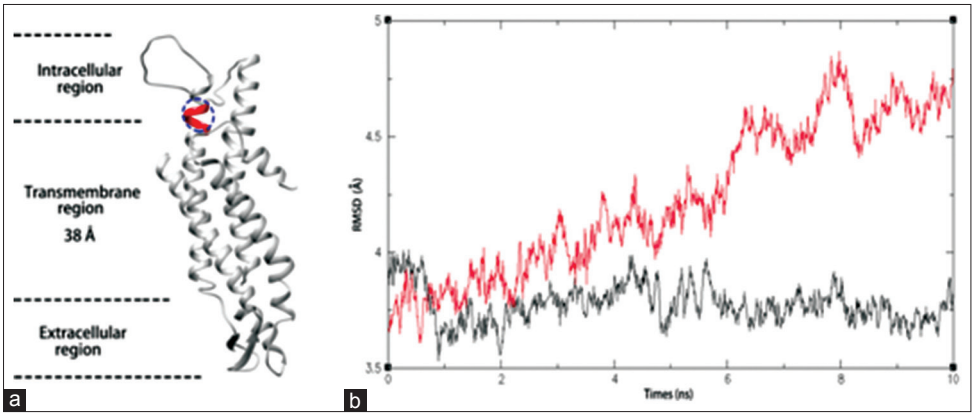

Figure 2: Molecular dynamics simulation. (a) The illustration of mono connexin 50 protein/membrane complex models. The blue circle represents the lost region in connexin 50 mutant. (b) Simulation of molecular dynamics. The black curve denotes the structure dynamics of wild type and the red curve denotes mutants. X-axis is the time of simulation and Y-axis is the root-mean-square deviation of atoms.

To date, about 28 *GJA8* mutations have been reported in CC patients [Figure 1d]. The majority of these mutations (26/28) are missense substitutes although rare cases of nonsense and frameshift mutations (2/28) have also been reported [Supplementary Table 4]. These mutations occur at the NT, TM1 to TM4, E1 and E2, or CT,[27] but none has been reported on the CL domain [Figure 1d and Supplementary Table 4]. No correlation between the mutation types or mutant region and the cataract phenotypes were observed. *In vitro*, functional analysis showed that these mutations triggered the formation of cataracts either through loss of normal channel functions (loss of function, altered gating, or reduced channel numbers) or gain of abnormal functions (gain of hemichannel function and formation of cytoplasmic accumulations).[9,27] The in-frame deletion reported here was first ever detected in the intracellular loop [Figure 1d and Supplementary Table 4] and its likely pathogenicity indicated the functional importance of the deleted sequence in the Cx50 gap junction protein. The structure modeling here showed that the deletion destabilized the structure of Cx50 protein channel. Thus, it is supposed that the mutation causes cataracts in the Chinese family as a dominant-negative function mutation due to impaired function of the channel or reduced number of normal channels.

In recent several years, great advances have been achieved in NGS and targeted genomic enrichment technologies. The combination of these two technologies has shown considerable potential and value in clinical applications, especially in genetic diagnosis of highly heterogeneous rare genetic diseases.[28] First, targeted sequencing of a small proportion of the genome (about 1/1000–1/100 of the genome) could reduce the sequencing cost to a level acceptable in clinical context. Second, the flexibility of targeted gene panel design and the availability of deep sequencing depth on NGS allow to simultaneously sequence all known genes for certain genetic disease and to comprehensively analyze SNVs, small InDels, and copy number variations at a high accurate level. Here, we performed targeted sequencing of 45 genes involved in CC (mainly in nonsyndromic CC) to explore the utility of targeted NGS sequencing for genetic diagnosis of ADCC. The high depth and completeness of sequences coverage for these 45 genes, as well as the readily identification of potential causative mutation, indicate that the targeted genes sequencing using NGS provides a tool for genetic diagnostics of nonsyndromic CC. More importantly, this method could be expanded to all CC with the addition of more CC genes in target panel.

However, a major limitation of this approach is that if the panel does not include genes responsible in tested patients, mutations will not be detected. Hence, the panel used needs to be updated when new genes are implicated in the disease. Another problem of the method is that some deep intronic mutations or mutations affecting regulatory elements may not be detected, which needs to be solved.

In conclusion, clinical molecular diagnosis of CC, particularly for ADCC, remains a challenge because of highly genetic and clinical heterogeneity. In this study, by combined NGS and targeted genomic enrichment technology, we identified a novel 15 deletion in a highly conserved region of CL domain of the *GJA8* gene associated with cataracts in a three-generation Chinese family with ADCC (mutations have never reported in CL domain before). Evidence supports a pathogenic role of the deletion in the family. More importantly, protein modeling indicates a dominant-negative impact of the deletion on the protein function. Our results demonstrate targeted genes sequencing on NGS as a useful tool for molecular diagnosis of CCs.

Acknowledgments

This work was supported by the experimental facilities and reagents of the BGI-Shenzhen, China. We would like to thank all of the blood donors for their uncompensated contribution to this study. We wish to thank the staff of BGI-Guangzhou for all the assistance provided in the process of sample collections. We gratefully acknowledge the support from Jiu-Cheng Liu for his assist in figures editing.

Supplementary information is linked to the online version of the paper on the Chinese Medical Journal website.

Financial support and sponsorship

This work was supported by the experimental facilities and reagents of the BGI-Shenzhen, China.

Conflicts of interest

There are no conflicts of interest.

References

1. Hejtmancik JF. Congenital cataracts and their molecular genetics. Semin Cell Dev Biol 2008;19:134-49. doi: 10.1016/j.semcdb.2007.10.003.
2. Apple DJ, Ram J, Foster A, Peng Q. Elimination of cataract blindness: A global perspective entering the new millenium. Surv Ophthalmol 2000;45:S1-2.
3. Sun W, Xiao X, Li S, Guo X, Zhang Q. Exome sequencing of 18 Chinese families with congenital cataracts: A new sight of the NHS gene. PLoS One 2014;9:e100455. doi: 10.1371/journal.pone.0100455.
4. Holmes JM, Leske DA, Burke JP, Hodge DO. Birth prevalence of visually significant infantile cataract in a defined U.S. population. Ophthalmic Epidemiol 2003;10:67-74. doi: 10.1076/opep.10.2.67.13894.
5. Haargaard B, Wohlfahrt J, Fledelius HC, Rosenberg T, Melbye M. Incidence and cumulative risk of childhood cataract in a cohort of 2.6 million Danish children. Invest Ophthalmol Vis Sci 2004;45:1316-20. doi: 10.1167/iovs.03-0635.
6. Santana A, Waiswo M. The genetic and molecular basis of congenital cataract. Arq Bras Oftalmol 2011;74:136-42. doi: 10.1590/S0004-27492011000200016.
7. Shiels A, Bennett TM, Hejtmancik JF. Cat-map: Putting cataract on the map. Mol Vis 2010;16:2007-15.
8. Hejtmancik J, Kaiser-Kupfer M, Piatigorsky J. Molecular biology and inherited disorders of the eye lens. Vol. 8. New York: McGraw Hill; 2001. p. 6033-62.
9. Shiels A, Hejtmancik JF. Genetics of human cataract. Clin Genet 2013;84:120-7. doi: 10.1111/cge.12182.
10. Reddy MA, Francis PJ, Berry V, Bhattacharya SS, Moore AT. Molecular genetic basis of inherited cataract and associated

phenotypes. Surv Ophthalmol 2004;49:300-15. doi: 10.1016/j.survophthal.2004.02.013.
11. Gillespie RL, O'Sullivan J, Ashworth J, Bhaskar S, Williams S, Biswas S, *et al.* Personalized diagnosis and management of congenital cataract by next-generation sequencing. Ophthalmology 2014;121:2124-37.e1-2. doi: 10.1016/j.ophtha.2014.06.006.
12. Kondo Y, Saitsu H, Miyamoto T, Lee BJ, Nishiyama K, Nakashima M, *et al*. Pathogenic mutations in two families with congenital cataract identified with whole-exome sequencing. Mol Vis 2013;19:384-9.
13. Reis LM, Tyler RC, Muheisen S, Raggio V, Salviati L, Han DP, *et al.* Whole exome sequencing in dominant cataract identifies a new causative factor, CRYBA2, and a variety of novel alleles in known genes. Hum Genet 2013;132:761-70. doi: 10.1007/s00439-013-1289-0.
14. Liu G, Wei X, Chen R, Zhou H, Li X, Sun Y, *et al.* A novel mutation of the SLC25A13 gene in a Chinese patient with citrin deficiency detected by target next-generation sequencing. Gene 2014;533:547-53. doi: 10.1016/j.gene.2013.10.021.
15. Wei X, Ju X, Yi X, Zhu Q, Qu N, Liu T, *et al.* Identification of sequence variants in genetic disease-causing genes using targeted next-generation sequencing. PLoS One 2011;6:e29500. doi: 10.1371/journal.pone.0029500.
16. Li H, Durbin R. Fast and accurate short read alignment with Burrows-Wheeler transform. Bioinformatics 2009;25:1754-60. doi: 10.1093/bioinformatics/btp324.
17. Li R, Li Y, Fang X, Yang H, Wang J, Kristiansen K, *et al.* SNP detection for massively parallel whole-genome resequencing. Genome Res 2009;19:1124-32. doi: 10.1101/gr.088013.
18. McKenna A, Hanna M, Banks E, Sivachenko A, Cibulskis K, Kernytsky A, *et al.* The genome analysis toolkit: A MapReduce framework for analyzing next-generation DNA sequencing data. Genome Res 2010;20:1297-303. doi: 10.1101/gr.107524.110.
19. Kircher M, Witten DM, Jain P, O'Roak BJ, Cooper GM, Shendure J. A general framework for estimating the relative pathogenicity of human genetic variants. Nat Genet 2014;46:310-5. doi: 10.1038/ng.2892.
20. Biasini M, Bienert S, Waterhouse A, Arnold K, Studer G, Schmidt T, *et al.* SWISS-MODEL: Modelling protein tertiary and quaternary structure using evolutionary information. Nucleic Acids Res 2014;42:W252-8. doi: 10.1093/nar/gku340.
21. Maeda S, Nakagawa S, Suga M, Yamashita E, Oshima A, Fujiyoshi Y, *et al.* Structure of the connexin 26 gap junction channel at 3.5 A resolution. Nature 2009;458:597-602. doi: 10.1038/nature07869.
22. Wu EL, Cheng X, Jo S, Rui H, Song KC, Dávila-Contreras EM, *et al.* CHARMM-GUI membrane builder toward realistic biological membrane simulations. J Comput Chem 2014;35:1997-2004. doi: 10.1002/jcc.23702.
23. Essmann U, Perera L, Berkowitz ML, Darden T, Lee H, Pedersen LG. A smooth particle mesh Ewald method. J Chem Phys 1995;103:8577-93. doi: 10.1063/1.470117.
24. Goga N, Rzepiela AJ, de Vries AH, Marrink SJ, Berendsen HJ. Efficient algorithms for langevin and DPD dynamics. J Chem Theory Comput 2012;8:3637-49. doi: 10.1021/ct3000876.
25. Chen Y, Zhou Y, Lin X, Wong HC, Xu Q, Jiang J, *et al.* Molecular interaction and functional regulation of connexin50 gap junctions by calmodulin. Biochem J 2011;435:711-22. doi: 10.1042/BJ20101726.
26. Zou J, Salarian M, Chen Y, Veenstra R, Louis CF, Yang JJ. Gap junction regulation by calmodulin. FEBS Lett 2014;588:1430-8. doi: 10.1016/j.febslet.2014.01.003.
27. Beyer EC, Ebihara L, Berthoud VM. Connexin mutants and cataracts. Front Pharmacol 2013;4:1-14. doi: 10.3389/fphar.2013.00043.
28. Ng SB, Buckingham KJ, Lee C, Bigham AW, Tabor HK, Dent KM, *et al.* Exome sequencing identifies the cause of a mendelian disorder. Nat Genet 2010;42:30-5. doi: 10.1038/ng.499.

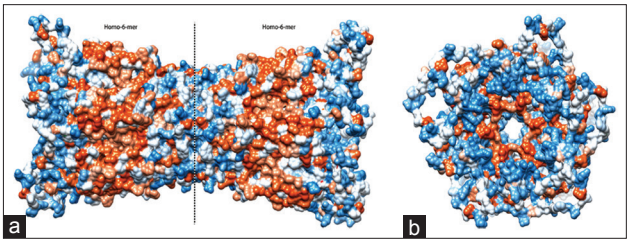

Supplementary Figure 1: (a and b) The overall structure of the connexin 50 channel model in hydrophobicity surface representation.

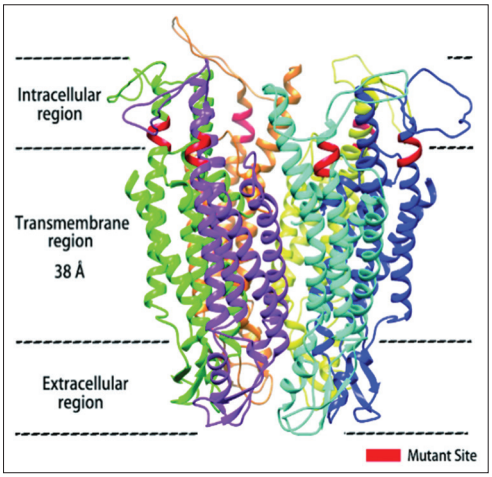

Supplementary Figure 2: The illustration of homo-6-mer connexin 50 protein/membrane complex models.

Supplementary Table 1: Primers for PCR amplification of exons of candidate genes and the size of the PCR products

Gene	Exon	Primers sequence (5'–3')	Fragment size (bp)
GJA8	2	F*-GTGCACTACGTCCGCATG	298
		R†-CGAAGCAGTCCACCACATTG	
MAF	1	F-AGCTGGTGACCATGTCTGTG	407
		R-AGAACTAGCAAGCCCACACC	
		F-AACTGGCAATGAGCAACTCC	548
		R-GTGGTGGTGGTGGTGGTAGT	
		F-GAGCGAGGGAGCACATTG	352
		R-CCGGTTCCTTTTTCACTTCA	
		F-CCGCACTACCACCACCAC	432
		R-CTGGTTCTTCTCCGACTCCA	
EPHA2	1	F-GACCAAGCTGAAACCGCTTA	684
		R-TACCAGGCTCAGAGATCCCT	
NHS	1	F-AGGCAAGGTGAGCAGAGAAG	764
		R-CGCAGAAACCCATAGCCTG	

*F: Forward primers; †R: Reverse primers; PCR: Polymerase chain reaction.

Supplementary Table 2: Gene (exons) with poor sequencing coverage and the associated diseases

Gene	Related cataracts	Exon	Size (bp)	GC content (%)	Sequencing depth (x)	Coverage rate (%)	Uncovered sequences		
							Region	Length (bp)	Percentage of all exons
EPHA2	#116600, cataract 6, multiple types, AD	EX1	240	74.17	29.70	54.12	c.1_85	85	2.14
BFSP1	#611391, cataract 33, AR	EX1	417	76.13	100.89	99.73	c.1_377	377	18.87
ABHD12	#612674, polyneuropathy, hearing loss, ataxia, retinitis pigmentosa, and cataract, AR	EX1	470	78.13	96.43	95.29	c.1_191	191	15.72
MAF	#610202, cataract, pulverulent or cerulean, with or without microcornea, AD	EX1	1941	69.65	72.14	77.28	c.1_1118	1118	42.24
CTDP1	#604168, congenital cataracts, facial dysmorphism, and neuropathy, AR	EX1	461	78.09	5.30	29.30	c.1_314	314	8.37
NHS	#302200, cataract 40, X-linked, XD	EX1	903	70.99	79.55	74.51	c.1_565	565	6.45

AR: Autosomal recessive; AD: Autosomal dominant; XD: X-linked dominant.

Supplementary Table 3: Variants detected in the 45 cataract genes in the proband

Gene	Transcript	Variant	Hom/ Het	Reads	Mutation type	Gene region	Functional region	rsID*	Frequency in dbSNP†	Frequency in HapMap‡	Frequency in 1000 genomes§	Frequency in 1100 exomes‖
SLC16A12	NM_213606	c.49 T>G	Het	C99/103A;202	SNV	CDS1	Missense	rs3740030	0.163	0.38	0.1538	0.3641
PITX3	NM_005029	c.285 C>T	Het	A25/22G;47	SNV	CDS2	Synonymous	rs2281983	0.43	0	0.424	0.3795
BEST1	NM_001139443	c.39 C>A	Hom	A142;142	SNV	CDS1	Synonymous	rs1109748	0.075	0.547	0.1474	0.5333
BEST1	NM_001139443	c.1428 T>C	Hom	C249/1T;250	SNV	CDS8	Synonymous	rs1800009	0	0	0.3553	0.7638
JAM3	NM_032801	c.978−3 T>C	Het	C106/142T;248	SNV	Intron7	Splice	rs610382	0.498	0.434	0.402	0.4342
GJA3	NM_021954	c.1017 G>A	Het	T41/19C;60	SNV	CDS1	Synonymous	rs11617415	0.371	0	0.3736	0.1949
GJA3	NM_021954	c.895 C>A	Hom	T103;103	SNV	CDS1	Missense	rs968566	0.966	0	0.967	1
CNBP	NM_001127192	c.156 C>T	Het	A108/86G	SNV	CDS2	Synonymous	rs4303883	0.381	0.277	0.2115	0.2308
CTDP1	NM_004715	c.978 G>A	Het	A127/122G;249	SNV	CDS7	Synonymous	rs599554	0.326	0.175	0.283	0.1128
CTDP1	NM_004715	c.1461 G>A	Het	A54/28G;82	SNV	CDS8	Synonymous	rs2126082	0.304	0	0.2756	0.1026
CTDP1	NM_004715	c.2817 T>C	Hom	C33;33	SNV	CDS13	Synonymous	rs626169	0.846	0.993	0.8672	0.9949
EPHA2	NM_004431	c.2874 C>T	Het	A42/49G;91	SNV	CDS17	Synonymous	rs3754334	0.355	0.226	0.326	0.241
EPHA2	NM_004431	c.1983 C>T	Het	A77/94G;171	SNV	CDS11	Synonymous	rs10907223	0.267	0.206	0.2024	0.1949
EPHA2	NM_004431	c.987 C>T	Het	A27/35G;62	SNV	CDS5	Synonymous	rs2230597	0.433	0.184	0.4158	0.2564
BFSP1	NM_001195	c.1749 A>G	Hom	C250;250	SNV	CDS8	Synonymous	rs6080718	0	0.358	0.5403	0.4154
BFSP1	NM_001195	c.1500 G>A	Het	T109/141C;250	SNV	CDS8	Synonymous	rs6136118	0.431	0.453	0.4295	0.4615
BFSP1	NM_001195	c.1033 G>A	Het	T102/108C;210	SNV	CDS7	Missense	rs6080719	0.378	0.489	0.3608	0.4564
BFSP1	NM_001195	c.90 G>A	Het	T2/3C;5	SNV	CDS1	Synonymous	snp105	0	0	0	0
ABHD12	NM_015600	c.1068 T>C	Hom	G211;211	SNV	CDS12	Synonymous	rs10966	0.31	0	0.3581	0.516
CRYAA	NM_000394	c.6 C>T	Hom	T149;149	SNV	CDS1	Synonymous	rs872331	0.276	0.03	0.315	0.2278
CRYBB3	NM_004076	c.337 C>G	Hom	G144;144	SNV	CDS4	Missense	rs9608378	0.456	0.867	0.4908	0.8718
CRYBB2	NM_000496	c.449+9 G>A	Hom	A96;96	SNV	Intron5	Splice	rs4049505	0	0	0.6145	0.9026
CRYBB2	NM_000496	c.483 G>A	Het	A67/79G;146	SNV	CDS5	Synonymous	rs8140949	0.412	0	0.3819	0.4923
CRYBA4	NM_001886	c.171 T>C	Hom	C128;128	SNV	CDS3	Synonymous	rs5761637	0.844	0	0.848	0.9949
CRYGD	NM_006891	c.285 A>G	Hom	C249;249	SNV	CDS3	Synonymous	rs2305430	0.626	0.453	0.6392	0.3846
CRYGD	NM_006891	c.51 T>C	Het	G37/40A;77	SNV	CDS2	Synonymous	rs200375285	0	0.518	0.435	0.2974
FYCO1	NM_024513	c.3924 C>T	Hom	A194;194	SNV	CDS13	Synonymous	rs1463680	0.739	0.956	0.7473	0.8114
FYCO1	NM_024513	c.2036 C>T	Het	A68/68G;136	SNV	CDS7	Missense	rs3796375	0.489	0.519	0.4203	0.3808
FYCO1	NM_024513	c.1335 G>A	Het	T101/140C;241	SNV	CDS7	Synonymous	rs3796376	0.315	0.562	0.3168	0.3203
FYCO1	NM_024513	c.962 G>C	Het	G60/84C;144	SNV	CDS7	Missense	rs3733100	0.499	0.489	0.457	0.3879
FYCO1	NM_024513	c.749 G>A	Hom	T219;219	SNV	CDS7	Missense	rs4683158	0	1	0.8498	0.8932
FYCO1	NM_024513	c.267 C>A	Hom	T249;249	SNV	CDS3	Synonymous	rs4682801	0.622	1	0.6667	0.8114
BFSP2	NM_003571	c.603 G>A	Het	A84/129G;213	SNV	CDS3	Synonymous	rs2276737	0.495	0.519	0.4277	0.4513
SLC33A1	NM_004733	c.512 A>G	Het	C113/137T;250	SNV	CDS1	Missense	rs3804769	0.174	0.226	0.1722	0.2278
EYA1	NM_172058	c.1755 T>C	Het	G51/42A;93	SNV	CDS16	Synonymous	rs10103397	0.497	0.407	0.4267	0.388
EYA1	NM_172058	c.1278 C>T	Het	A135/115G;250	SNV	CDS12	Synonymous	rs4738118	0.399	0.455	0.2811	0.4614
EYA1	NM_172058	c.813 A>G	Hom	C248;248	SNV	CDS7	Synonymous	rs1445398	0.034	0.224	0.0632	0.1747
TDRD7	NM_014290	c.33 A>G	Hom	G249;249	SNV	CDS1	Synonymous	rs1381532	0.322	0.299	0.3114	0.2811

Contd...

Supplementary Table 3: Contd...

Gene	Transcript	Variant	Hom/ Het	Reads	Mutation type	Gene region	Functional region	rsID*	Frequency in dbSNP†	Frequency in HapMap‡	Frequency in 1000 genomes§	Frequency in 1100 exomes‖
TDRD7	NM_014290	c.449 T>C	Hom	C243/5T;248	SNV	CDS3	Missense	rs2045732	0.322	0.281	0.3114	0.2776
NHS	NM_198270	c.3955 T>C	Het	C128/121T;249	SNV	CDS6	Missense	rs3747295	0.469	0.25	0.1374	0.1692
MAF	NM_005360	c.–1637_−1639 delGGC	Het	W34/M14;48	Deletion	5-UTR	5-UTR	_	No_frequency	Not_in_HapMap	0	0.4744
GJA8	NM_005267	c.426_440 delGCTG GA GGGGACCCT	Het	W169/M78;247	Deletion	CDS1	CDS	_	No_frequency	Not_in_HapMap	0	0
RAB3GAP2	NM_012414	c.812−6 delT	Het	W67/M68;135	Deletion	Intron9	Splice	_	No_frequency freq	Not_in_HapMap	0	0.3154

*NCBI dbSNP ID; †Allele frequency in NCBI dbSNP; ‡Allele frequency in HapMap; §Allele frequency in 1000 genome project; ‖Allele frequency in BGI in-house control exomes. dbSNP: Single nucleotide polymorphism database; SNV: Single nucleotide variant; UTR: Untranslated regions; CDS: Coding sequence; BGI: Beijing Genomic Institute.

Supplementary Table 4: Reported connexin 50 mutants and associated cataracts

Mutation	Amino acid change	Location	Cataract types	Inheritary	Family origin	References
68G>C	R23T	NT*	Progressive dense nuclear	Autosomal dominant	Iranian	Willoughby *et al*. 2003
92T>C	I31T	M1†	Nuclear cataract	Autosomal dominant	Chinese	Wang *et al*. 2009
116C>G	T39R	M1	Cataract and microcornea and iris hypoplasia	Autosomal dominant	Chinese	Sun *et al*. 2011
131T>A	V44E	M1	Cataract and microcornea	Autosomal dominant	Indian	Devi and Vijayalakshmi 2006
131T>C	V44A	M1	Suture-sparing nuclear cataracts	Autosomal dominant	Chinese	Zhu *et al*. 2014
134G>C	W45S	M1	Jellyfish-like bilateral and microcornea	Autosomal dominant	Indian	Vanita *et al*. 2008b
136G>A	G46R	M1	Complete and microcornea	Autosomal dominant	Chinese	Sun *et al*. 2011
137 G>T	G46V	M1	Total cataract	Autosomal dominant	Pakistani	Minogue *et al*. 2009
139G>A	D47N	E1‡	Nuclear pulverulent	Autosomal dominant	British	Arora *et al*. 2008; Wang *et al*. 2011
139G>T	D47Y	E1	Nuclear cataract	Autosomal dominant	Chinese	Lin *et al*. 2008
139G>C	D47H	E1	Nuclear cataract	Autosomal dominant	Chinese	Li *et al*. 2013
142G>A	E48K	E1	Zonular nuclear pulverulent	Autosomal dominant	Pakistani	Berry *et al*. 1999
191T>G	V64G	E1	Nuclear	Autosomal dominant	Chinese	Ma *et al*. 2005
218C>T	S73F	E1	Dense and "star-shaped," various locations in the nucleus or the poles	Autosomal dominant	Danish	Hansen *et al*. 2009
235G>C	V79L	M2§	"Full moon" Y-sutural opacity	Autosomal dominant	Indian	Vanita *et al*. 2006
262C>T	P88S	M2	Zonular pulverulent	Autosomal dominant	British	Shiels *et al*. 1998
262C>A	P88Q	M2	Lamellar pulverulent	Autosomal dominant	British	Arora *et al*. 2006
262C>A	P88Q	M2	"Balloon-like" Y-sutural opacities	Autosomal dominant	Indian	Vanita *et al*. 2008a
264C>T	P88T	M2	Total cataract	Autosomal dominant	Chinese	Ge *et al*. 2014
565C>T	P189L	E2‖	Cataract and microcornea	Autosomal dominant	Danish	Hansen *et al*. 2007
593G>A	R198Q	E2	Cataract and microcornea	Autosomal dominant	Indian	Devi and Vijayalakshmi 2006
592C>T	R198W	E2	Cataract and microcornea	Autosomal dominant	Chinese	Hu *et al*. 2010
601G>A	E201K	E2	Perinuclear cataracts	Autosomal dominant	Chinese	Su *et al*. 2013
670insA	203fs	E2	Cataract	Autosomal recessive	Indian	Ponnam *et al*. 2007
773C>T	S258F	CT¶	Nuclear	Autosomal dominant	Chinese	Gao *et al*. 2010
776insG	fs	CT	Triangular	Autosomal recessive	Germany	Schmidt *et al*. 2008
836C>A	S259Y	CT	–	Autosomal dominant	Danish	Hansen *et al*. 2009
827C>T	S276F	CT	Nuclear pulverulent	Autosomal dominant	Chinese	Yan *et al*. 2008
905T>C	L281C	CT	Lamellar/zonular	Autosomal dominant	Indian	Kumar *et al*. 2011

*Cytoplasmic amino-terminal, †First transmembrane domain, ‡Extracellular loop 1, §Second transmembrane domain, ‖Extracellular loop 2, ¶Cytoplasmic carboxy-terminal. NT: N-terminal; CT: C-terminal.